SILKY SHARK POPULATION TREND IN THE INDIAN OCEAN DERIVED FROM ITS ASSOCIATIVE BEHAVIOUR WITH FLOATING OBJECTS

Alexandra Diallo[1], Mariana Travassos Tolotti[1,*], Philippe Sabarros[1], Laurent Dagorn[1] Jean-Louis Deneubourg[2], Hilario Murua[3], Jon Ruiz Gondra[4], Lourdes Ramos Alonso[5], José Carlos Báez[5], Francisco J. Abascal Crespo[5], Pedro José Pascual Alayón[5] and Manuela Capello[1]

[1]Institut de Recherche pour le Developpement (IRD), UMR MARBEC (IRD, Ifremer, Univ. Montpellier, CNRS), Sete - France

[2]Unité d'Ecologie Sociale, Université Libre de Bruxelles, Campus de la Plaine, Bruxelles - Belgium

[3]ISSF, International Seafood Sustainability Foudation, Washington DC - USA

[4]AZTI, Marine Research Division, Sukarrieta – Spain

[5]Instituto Español de Oceanografía - Spain

Abstract

Silky sharks (*Carcharhinus falciformis*) figure among the main pelagic shark species caught by the industrial tropical tuna purse-seine fisheries. However, this data was not used so far for estimating their population trends. In this study, using data from the European tropical tuna purse seine fishery, we provide an abundance trend for the silky shark, based on the associative behavior of this species with floating objects (FOBs). Two models were used, describing the dynamics of sharks associated to floating objects (FOBs) in a social and in a non-social case. The parameters estimates of the models were obtained by fitting the distribution of the number of sharks caught per set. The relative abundance indices were derived for the Seychelles area and the Mozambique Channel. For both areas, an upward trend was observed. In the Seychelles area, the abundance index increased by a factor of 3 from 2006 to 2018 and in the Mozambique Channel the increase reached a factor of 15. This modeling approach could be extended to other bycatch species to generate population trends and could be useful for future stock assessment analyses.

Keywords: Abundance index; *Carcharhinus falciformis*; social behavior; tropical tuna purse seine fishery

1. Introduction

Ranked as vulnerable to near threatened on the IUCN red list, the silky shark (*Carcharhinus falciformis*) is a pelagic species distributed in tropical waters and vulnerable to tropical tuna fisheries. It is mainly caught as bycatch by pelagic longlines and gillnets, being also commonly captured by purse seiners (Fonteneau et al., 2013; Restrepo et al., 2017).

The European tropical purse seine fishery is currently one of the most modern and powerful fisheries in the world, accounting for 64% of the 4.7 million tons of tunas caught worldwide every year (Justel-Rubio et al., 2017). Two main types of tuna schools are targeted by the purse seiners: (i) free-swimming schools, generally monospecific, composed of larger individuals; and (ii) schools associated with floating objects (FOBs), that are multispecific and

composed of smaller individuals. To date, 40 to 60% of the world's annual tropical tuna catches come from fishing sets on FOBs and between 50 and 100 thousands FOBs are deployed worldwide every year (Dagorn et al., 2013a; Filmalter et al., 2013; Fonteneau et al., 2013).

There are between 2.8 to 6.7 times more bycatch on FOB-associated sets than on free-swimming schools sets (Dagorn et al., 2013b). Elasmobranches account for about 5% of the total tuna biomass caught under FOBs, with the silky shark representing 90% of the catches of this group (Gilman, 2011). Recent estimates suggest that the total annual catch of silky sharks within the purse seine tropical tuna fisheries can reach up to 1,280 tons in the Indian Ocean and up to 39 tons in the Atlantic (Restrepo et al., 2017). Information regarding the state of the population of silky sharks is needed in order to assess the impact of the purse seine fisheries on this species.

The aim of this study is to develop a methodology to derive an abundance index for the silky shark using catch data from the European tropical tuna purse seine fishery in the Indian Ocean. Two main objectives are targeted: (i) determine the association dynamics of silky sharks around FOBs through model comparisons; and (ii) derive an abundance index and draw an abundance trend based on the exchanges of individuals between the FOB-associated population and an external pool of sharks using the parameters estimated by the best models describing the association dynamics.

2. Data preparation

Observer data from the European tropical tuna purse seine fleet in the Indian Ocean (French and Spanish), spanning from 2005 and 2018, were used in the analyses (Figure 1). The data was provided by Ob7[1], AZTI Tecnalia and IEO[2]. Only sets on floating objects (FOBs) were considered in the analyses. The total number of silky sharks caught under a single FOB set was used to classify catch events, starting from sets with zero silky shark occurrence up to sets with 20 silky sharks. These sets corresponded to more than 95% of the total data. The proportion of each catch event in relation to the total number of FOB sets was then calculated and represented in the form of histograms for statistical units of time and space in which the local population of the silky shark could be considered homogeneous. Two areas matching stock assessment regions were defined: the Mozambique Channel and the Seychelles area (Figure 2). Based on the spatial movements and residence time of silky sharks around FOBs (Filmalter et al., 2015, 2011), the temporal window was defined as 3 months and set to match fishing quarters: December-January-February (Q1), March-April-May (Q2), June-July-August (Q3) and September-October-November (Q4).

[1] Observatoire des Ecosystèmes Pélagiques Tropicaux exploités

[2] Instituto Español de Oceanografía

Fixing a minimum threshold of 20 sets, the available observers data allowed defining a total of 50 statistical units were defined, 11 in the Mozambique Channel and 39 in the Seychelles area. In the Mozambique Channel, the statistical units were mostly represented by Q2 and spanned from 2007 and 2018. In the Seychelles area the statistical units spanned from Q1 2007 to Q3 2018. An example of statistical unit with its respective catch events histogram is shown in Figure 3.

Sample size varied significantly from one statistical unit to another, mainly due to the higher observer coverage in recent years. To detect the effect of this sampling variability on the abundance index value, bootstrap resampling was conducted (Efron and Tibshirani, 1994). Each statistical unit with more than 100 fishing sets was down-sampled in 50 iterations (Figure 4). The size of the down-samples was defined as the mean size of all statistical units with less than 100 fishing sets for each area. The resulting down-samples size was 47 for the Mozambique Channel and 61 for the Seychelles area. The analyses described in the following sections were applied to both the original and down-sampled data.

3. Modeling silky shark's dynamics around FOBs

Two models were used to describe the dynamics of silky sharks around FOBs. In the first model, silky sharks were considered to display social behavior, while in the second one they were considered to be non-social. The social behavior was modeled as a change in the residence time of a silky shark associated with a FOB when a certain number of congeners are present. This approach follows the postulate that the probability of a silky shark to leave a FOB will decrease if other silky sharks are also present at the same FOB. For the non-social scenario we hypothesized that the presence of congeners will not influence the residence time.

3.1. Social model

Considering X a discrete random variable representing the associated population of sharks at a FOB and Ω a threshold of sociability, the dynamics of X was modeled according to the conceptual scheme shown in Figure 5. At each time step, a FOB with a population of X=i can gain a shark with a constant probability α, and can lose a shark with a probability $i\ \lambda_1$, if $i \leq \Omega$, and a probability $i\ \lambda_2$, if $i > \Omega$, with $\lambda_1 > \lambda_2$. Considering that the system is at equilibrium, the probability $P\ (X{=}i)$ for a FOB to be at a state i is:

$$\begin{cases} P(0) = \dfrac{1}{\sum_{i=0}^{\Omega} \frac{1}{i!}\left(\frac{1}{{l_1}^i} - \frac{{l_2}^{\Omega}}{{l_1}^{\Omega}}\ \frac{1}{{l_2}^i}\right) + \frac{{l_2}^{\Omega}}{{l_1}^{\Omega}} e^{-(1/l_2)}} \\ P_{i \leq \Omega}(X = i) = \dfrac{1}{i!\ {l_1}^i}\ P(0) \\ P_{i > \Omega}(X = i) = \dfrac{1}{i!}\ \dfrac{1}{{l_1}^{\Omega} {l_2}^{i-\Omega}}\ P(0) \end{cases} \quad \text{(Equation 1)}$$

With $\frac{\lambda_1}{\alpha} = l_1$ and $\frac{\lambda_2}{\alpha} = l_2$.

3.2. Non-social model

The non-social model corresponds to the social model shown in Equation 1 with $l_1 = l_2 = l$ (or $\Omega = 0$). Similarly to the social model, the probability for a FOB to gain a shark is constant and is represented by α. In this case the probability $P(X=i)$ becomes:

$$\begin{cases} \mathrm{P}(0) = e^{-(1/l)} \\ P(X=i) = \frac{1}{i!}\left(\frac{1}{l}\right)^i P(0) \end{cases} \quad \text{(Equation 2)}$$

By substituting (0) into the second equation we find $(X=i) = \frac{1}{i!}\left(\frac{1}{l}\right)^i e^{-(1/l)}$, which is equivalent to a Poisson probability density function $X \sim P\left(\frac{1}{l}\right)$.

3.3. Fitting the probability functions

The distributions of catch events calculated for each statistical unit were fitted with the probability functions shown in Equations 1 and 2. Aikaike Information Criterion (AIC), qq-plots and significance of the model parameters were used to determine which model (social and non-social) best described the observed distributions. For the social model, fits were also used to define the best Ω value. A total of 5 social models were tested with $\Omega \in [1,5]$. The fits were conducted using Maximum Likelihood for non-linear models, through the nlsLM function of the minpack.lm package in R. Models with non-significant parameters were excluded from the comparisons. For the remaining models, best fits were chosen based on AIC values and qq-plots.

For 3 of the 39 statistical units from the Seychelles area no model could be fitted, as all parameters were not significant. Most catch event distributions were best fitted by the social model with a social threshold (Ω) equal to 1, reaching 55% of statistical units from the Mozambique Channel and 69% from the Seychelles area (Table 1). Together, the best-fitted social models ($\Omega \in [1,3]$) described 94% of all distributions. The models with a social threshold of 4 and 5 were never classified as best fits because one of their parameters (l_2) was always non-significant. The Poisson function (non-social model) only provided the best fit for 3 distributions. An example of a comparative analysis between two fits is shown in Figure 6.

Table 1. Proportion of statistical units best fitted by each model. P= Poisson (non-social), S= social.

Area	Mozambique Channel			Seychelles			
Function	P	S Ω=1	S Ω=2	P	S Ω=1	S Ω=2	S Ω=3
Best fit (%)	**9**	**55**	**36**	**6**	**69**	**22**	**3**

4. Deriving an abundance index for the silky shark

Considering a group of N_{FOB} and a population of N_s silky sharks, the dynamics of the number of sharks X_j at FOB *j* (Figure 5) can be expressed as the following differential equation:

$$\frac{dX_j}{dt} = \mu_j X_e - \theta_j X_j \qquad \text{(Equation 3)}$$

where Xe is the unassociated population, μ the individual probability for a shark to join a FOB and θ the individual probability for a shark to leave a FOB. The social interactions are accounted at the level of the individual probability to leave a FOB (similar to the model shown in Eq. 1), considering that the probability θ_j is equal to θ_1 or θ_2 depending if the associated population is lower or higher than Ω. The total associated population can be written as $X_a = \sum_{j=1}^{N_{FOB}} X_j$ with N_{FOB} being the number of FOBs in the system and $N_s = X_e + X_a$ the total population of sharks. Notice that it is possible to relate the models in Equation 1 and Equation 3 considering $\theta_1 = \lambda_1$ and $\alpha = \mu X_e$.

The evolution in time of the associated population X_a can be written as:

$$\frac{dX_a}{dt} = N_{FOB}\,\mu\,X_e - \theta_1 X_\Omega - \theta_2 X_S \qquad \text{(Equation 4)}$$

with X_Ω being the total number of sharks associated to FOBs j having $X_j \leq \Omega$, i.e. the total number of sharks associated with FOBs below the sociality threshold. Similarly, $X_S = X_a - X_\Omega$ corresponds to the total number of sharks associated to FOBs j having $X_j > \Omega$. At equilibrium, Equation 4 can be written as:

$$X_e = \frac{\theta_1}{N_{FOB}\,\mu} X_\Omega + \frac{\theta_2}{N_{FOB}\,\mu} X_s \qquad \text{(Equation 5)}$$

Substituting Equation 5 into $N_s = X_e + X_a$ and considering that $X_a = X_\Omega + X_S$, the total population of sharks can be expressed as:

$$N_s = \left[1 + \frac{\theta_1}{N_{FOB}\,\mu}\right] X_\Omega + \left[1 + \frac{\theta_2}{N_{FOB}\,\mu}\right] X_s \qquad \text{(Equation 6)}$$

Note that, in the above equation, the total number of FOBs is a key variable to assess shark abundance. Quantifying FOB numbers remains a challenge and, although efforts have been made (Dagorn et al., 2013a; Maufroy et al., 2015), available estimates are uncertain. To simplify this problem, the total number of FOBs could be expressed by an index of FOB density as $N_{FOB} = f\, i_{NFOB}$, with i_{NFOB} being the FOB-density index and f being a coefficient relating the FOB-density index with the total number of FOBs.

The total shark population associated below/above the social threshold can be expressed as:

$$\begin{cases} X_{\Omega} = N_{FOB} \sum_{i \leq \Omega} i\, P(X = i) = N_{FOB}\, \Psi(X_{\Omega}) \\ X_{S} = N_{FOB} \sum_{i > \Omega} i\, P(X = i) = N_{FOB}\, \Psi(X_{S}) \end{cases} \qquad \text{(Equation 7)}$$

where $\Psi(\mathrm{X}_{\Omega}) = \sum_{\mathrm{i} \leq \Omega} \mathrm{i}\, \mathrm{P}(\mathrm{X} = \mathrm{i})$ and $\Psi(\mathrm{X}_{\mathrm{S}}) = \sum_{\mathrm{i} > \Omega} \mathrm{i}\, \mathrm{P}(\mathrm{X} = \mathrm{i})$, with $\mathrm{P}(\mathrm{X} = \mathrm{i})$ being the probability to find a FOB occupied by $\mathrm{X} = \mathrm{i}$ sharks, see Equation 1. Substituting the FOB-density index and Equation 7 into Equation 6, we arrive at the following abundance index:

$$N_s = f\left[\Psi(X_{\Omega})(i_{NFOB} + \gamma') + \Psi(X_s)\left(i_{NFOB} + \frac{\gamma'}{c}\right)\right] \qquad \text{(Equation 8)}$$

with $\gamma' = \frac{\theta_1}{\mu f}$ and $c = \frac{\theta_1}{\theta_2} = \frac{l_1}{l_2}$

The values of $\Psi(\mathrm{X}_{\Omega})$, $\Psi(\mathrm{X}_{\mathrm{S}})$ and c can be obtained from the histograms of the number of sharks per FOB and the fits, and the FOB-density index $\mathrm{i}_{\mathrm{NFOB}}$ can be estimated.

Therefore, for each statistical unit corresponding to a given time t and area A, the above equation can be rewritten as:

$$\widehat{N}_{s|t,A} = f\left[\widehat{\Psi}_{t,A}(X_{\Omega})\left(\hat{i}_{NFOB|t,A} + \gamma'\right) + \widehat{\Psi}_{t,A}(X_s)\left(\hat{i}_{NFOB|t,A} + \frac{\gamma'}{\hat{c}_{|t,A}}\right)\right] \qquad \text{(Equation 9)}$$

This equation still has two unknowns: the coefficient f relating the FOB-density index with the total number of FOBs and γ', that also depends on the probabilities of a shark to leave and reach a FOB (θ_1 and μ, respectively).

Considering that f and γ' do not vary in time, it is possible to obtain trends in the relative abundance of silky sharks for the same area (relative to a reference time) according to different values of γ'. In the Mozambique Channel, the reference period was the March-April-May quarter (Q2) of 2007, while in the in Seychelles area the reference period was the June-July-August quarter (Q3) of 2006.

5. Deriving an abundance trend for the silky shark

For each statistical unit, a simple FOB-density index was derived based on records of FOBs encounters from observers' data. The index corresponded to the total number of random FOB encounters recorded by the observers, standardized by the sampling effort (total number of days at sea). A random encounter was defined as the encounter of a FOB of unknown ownership (i.e., a FOB of a fishing vessel/fleet different from the one of the observer).

Assuming a constant value of *f*, the abundance indices obtained for every quarter between 2006 and 2018, relative to the reference period of each area (denoted as REF below), were calculated as follows:

$$T = \frac{N_{S|t,A}}{N_{S|REF,A}} = \frac{\left[\hat{\Psi}_{t,A}(X_\Omega)(\hat{\imath}_{NFOB|t,A}+\gamma')+\hat{\Psi}_{t,A}(X_S)\left(\hat{\imath}_{NFOB|t,A}+\frac{\gamma'}{\hat{c}_{|t,A}}\right)\right]}{\left[\hat{\Psi}_{REF,A}(X_\Omega)(\hat{\imath}_{NFOB|REF,A}+\gamma')+\hat{\Psi}_{REF,A}(X_S)\left(\hat{\imath}_{NFOB|REF,A}+\frac{\gamma'}{\hat{c}_{|REF,A}}\right)\right]}$$

with t detonating a quarter in the interval $[2006,2018]$ (Equation 10)

The constant γ' in Equation 10 was considered as a parameter and a large range of values were tested [10^{-5}:10^{15}] for all statistical units and their down-sampled replicates. The results in Figure 8 show two main trends, one for small values of γ' and other for large values. An intermediate zone could be identified between log(γ')= 0 and log(γ')= 3, where the index shows a larger variability.

Independently of the value of γ', the temporal trends of the relative abundance index increased with time (Figure 8). In the Seychelles area, the abundance index increased by a factor of 3 from 2006 to 2018 (Figure 9) and in Mozambique Channel the increase much higher, reaching a factor of 15 (Figure 10).

6. Remarks

By modeling silky shark's dynamics around FOBs we observed that 94% of the statistical units were best explained by a social behavior. In summary, silky sharks would stay associated with a FOB for a shorter period of time unless other congeners are associated and their corresponding "social threshold" was reached. The majority of cases (66%) were best explained by a social threshold of 1. This means that as soon as two sharks share a FOB, their residence time would increase. However, it is possible that this kind of binary response does not translate the reality of the departure probability. Instead, a continuous departure probability, monotonically decreasing with the number of sharks, could better describe the social dynamics. Finding a way to include these laws when fitting the probability functions to the distribution of catch events could provide better fits and a more precise abundance index.

Field experiments can also shed a light into the associative behavior of silky sharks. Studies using photography and video analysis, as well as acoustic telemetry, have described intraspecific interactions and movements of a range of species (Capello et al., 2011; Filmalter et al., 2015; Mourier et al., 2012; Robert et al., 2013). These approaches could broaden the knowledge on silky sharks' social behavior around FOBs and help validate the social model.

In the continuity of last year's work (Diallo et al., 2018), we were able to derive a decal abundance trend for the silky shark that takes into account the associative behavior of the species in two fishing areas of the Indian Ocean. The obtained trends followed the same increasing pattern, although the magnitude of the increase varied depending on the area. An increase on silky shark's population in the Indian Ocean could be a result of a combination of factors that took place as from 2010 (e.g. introduction of non-entangling FADs, Chagos MPA, shift of fishing effort due to piracy, Maldivian shark fishing ban). Nevertheless, it important to note that this abundance index is not a population estimate, which means that the observed upward trends should not be interpreted as an indication of a healthy population. Assumptions about stock status should not be made without quantitative estimates of the baseline population.

The magnitude of the increase on the abundance trends also varied depending on the value of γ' that was considered. Taking into account that $f \sim N_{FOB} \gg 1$ and that $\gamma' = \frac{\theta_1}{\mu f}$, the regime of large γ' could only occur for $\theta_1 \gg \mu$, i.e. if the probabilities of departure from the FOB are much higher than the probability to reach a FOB. Such information, which is not available at the moment, could be obtained from electronic experiments measuring residence and absence times of silky sharks in an array of FOBs. For the moment, the electronic tagging data recorded for silky sharks can only provide estimates of residence times (Filmalter et al., 2015). With these types of electronic tagging experiments, it would also be possible to test whether the assumption of a constant γ' (and thus constant probabilities to reach/depart from the FOB) holds. Indeed, external factors might equally play a role in the residence/absence times of silky sharks around FOBs. Juvenile silky sharks are believed to use FOBs as shelter to hide from predators or as feeding point (Bonfil, 2008; Filmalter et al., 2017). Therefore, the presence of prey, as well as inter-specific associations could influence the probabilities to reach/depart from FOBs. Environmental factors could also play a role, as their influence on the species' catch rates have been shown (Lennert-Cody et al., 2018; Lopez et al., 2017).

7. Conclusion

In summary, the social model appears to better explain the presence of silky sharks at FOBs. Further field experiments could give a finer understanding of the mechanisms underlying

silky shark's associative behavior, and also allow for a finer estimation of the model parameters. The model was nonetheless efficient in describing silky sharks' dynamics in a FOB environment, as well as in the first derivation of a relative abundance index. This modeling approach could be extended to other bycatch species to generate population trends and could be useful for future stock assessment analyses.

8. Acknowledgments

Diallo A received funding from Ob7 and from the European project CECOFAD2 (*Captures, Effort et Impacts sur l'écosystème des pêcheries thonières tropicales*). Data collection was ensured by Ob7, AZTI and IEO through observer programs conducted under European Data Collection Framework (EU/DCF) and under programs funded by the industry.

9. References

Bonfil, R., 2008. The Biology and Ecology of the Silky Shark,Carcharhinus Falciformis, in: Camhi, M.D., Pikitch, E.K., Babcock, E.A. (Eds.), Sharks of the Open Ocean. Blackwell Publishing Ltd., Oxford, UK, pp. 114–127.

Dagorn, L., Bez, N., Fauvel, T., Walker, E., 2013a. How much do fish aggregating devices (FADs) modify the floating object environment in the ocean? Fish. Oceanogr. 22, 147–153. doi:10.1111/fog.12014

Dagorn, L., Holland, K.N., Restrepo, V., Moreno, G., 2013b. Is it good or bad to fish with FADs? What are the real impacts of the use of drifting FADs on pelagic marine ecosystems? Fish Fish. 14, 391–415. doi:10.1111/j.1467-2979.2012.00478.x

Diallo, A., Tolotti, M.T., Sabarros, P., Dagorn, L., Deneubourg, J.-L., Capello, M., 2018. Can we derive an abundance index for the silky shark based on its associative behavior with floating objects? IOTC Work. Party Ecosyst. Bycatch IOTC-2018-WPEB14-32.

Efron, B., Tibshirani, R.J., 1994. An introduction to the bootstrap. CRC press.

Filmalter, J., Cowley, P., Forget, F., Dagorn, L., 2015. Fine-scale 3-dimensional movement behaviour of silky sharks Carcharhinus falciformis associated with fish aggregating devices (FADs). Mar. Ecol. Prog. Ser. 539, 207–223. doi:10.3354/meps11514

Filmalter, J.D., Capello, M., Deneubourg, J.L., Cowley, P.D., Dagorn, L., 2013. Looking behind the curtain: Quantifying massive shark mortality in fish aggregating devices. Front. Ecol. Environ. 11, 291–296. doi:10.1890/130045

Filmalter, J.D., Cowley, P.D., Potier, M., Ménard, F., Smale, M.J., Cherel, Y., Dagorn, L., 2017. Feeding ecology of silky sharks Carcharhinus falciformis associated with floating objects in the western Indian Ocean. J. Fish Biol. 90, 1321–1337. doi:10.1111/jfb.13241

Filmalter, J.D., Dagorn, L., Cowley, P.D., Taquet, M., 2011. First Descriptions of the Behavior of Silky Sharks, *Carcharhinus Falciformis,* Around Drifting Fish Aggregating Devices in the Indian Ocean. Bull. Mar. Sci. 87, 325–337. doi:10.5343/bms.2010.1057

Fonteneau, A., Chassot, E., Bodin, N., 2013. Global spatio-temporal patterns in tropical tuna purse seine fisheries on drifting fish aggregating devices (DFADs): Taking a historical perspective to inform current challenges. Aquat. Living Resour. 26, 37–48. doi:10.1051/alr/2013046

Gilman, E.L., 2011. Bycatch governance and best practice mitigation technology in global tuna fisheries. Mar. Policy 35, 590–609. doi:10.1016/j.marpol.2011.01.021

Justel-Rubio, A., Recio, L., Restrepo, V., 2017. A snapshot of the large scale tropical tuna

purse seine fishing fleets as of June 2017. Washington, D.C.

Lennert-Cody, C.E., Clarke, S.C., Aires-da-Silva, A., Maunder, M.N., Franks, P.J.S., Román, M., Miller, A.J., Minami, M., 2018. The importance of environment and life stage on interpretation of silky shark relative abundance indices for the equatorial Pacific Ocean. Fish. Oceanogr. 1–11. doi:10.1111/fog.12385

Lopez, J., Alvarez-Berastegui, D., Soto, M., Murua, H., 2017. Modelling the Oceanic Habitats of Silky Shark (Carcharhinus Falciformis), Implications for Conservation and Management. Indian Ocean Tuna Comm.

Maufroy, A., Chassot, E., Joo, R., Kaplan, D.M., 2015. Large-Scale Examination of Spatio-Temporal Patterns of Drifting Fish Aggregating Devices (dFADs) from Tropical Tuna Fisheries of the Indian and Atlantic Oceans. PLoS One 10, e0128023. doi:10.1371/journal.pone.0128023

Restrepo, V., Dagorn, L., Itano, D., Justel-Rubio, A., Moreno, G., Forget, F., 2017. A summary of bycatch issues and ISSF mitigation initiatives to-date in purse seine fisheries, with emphasis on FADs. Washington, D.C.

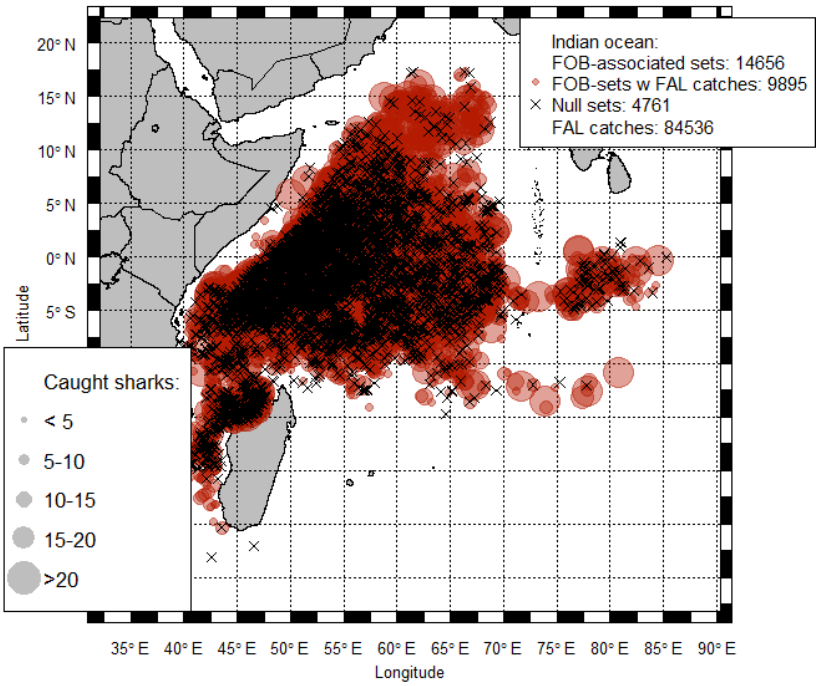

Figure 1. Silky shark captures by the European tropical tune purse seine fleet between 2005 and 2018. Crosses represent sets without any capture of silky sharks and circles are proportional to the number of sharks caught within a set.

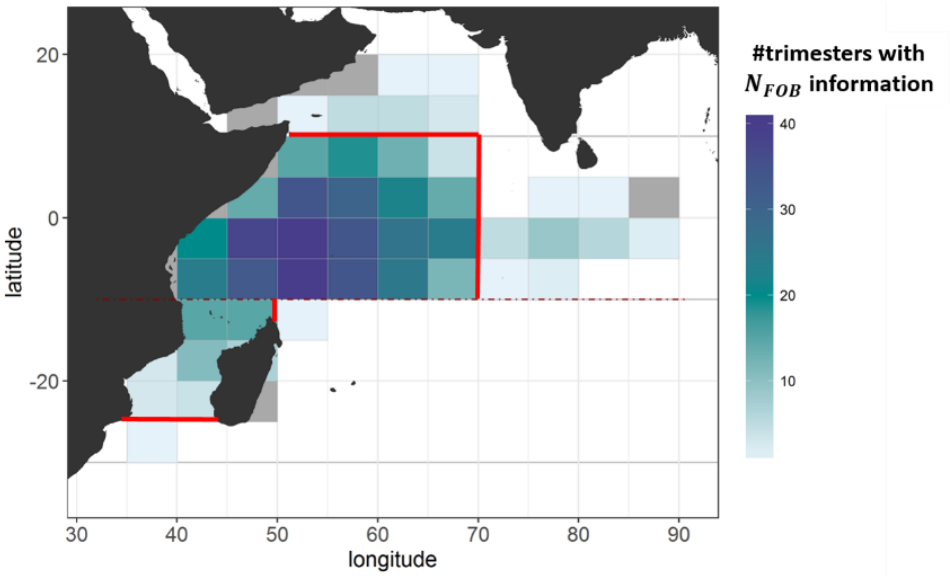

Figure 2. Delimitation of the study areas (red lines). Upper rectangle represents the Seychelles area and lower rectangle represents the Mozambique Channel area. The map also depicts the areas where the FOB-density index is available for the period of study.

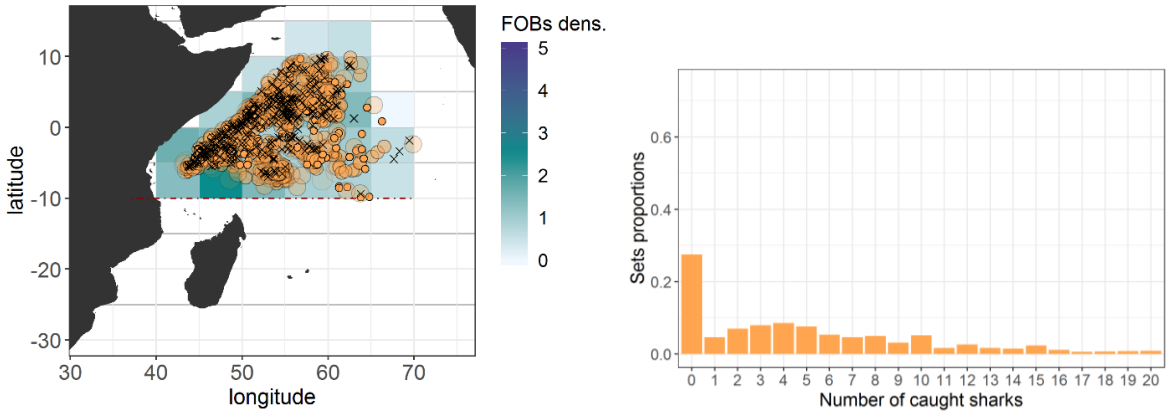

Figure 3. Example of a statistical unit. Left panel shows the spatial distribution of sets in the Seychelles area during the Set-Oct-Nov quarter (Q4) of 2017. Right panel shows the corresponding catch events histogram.

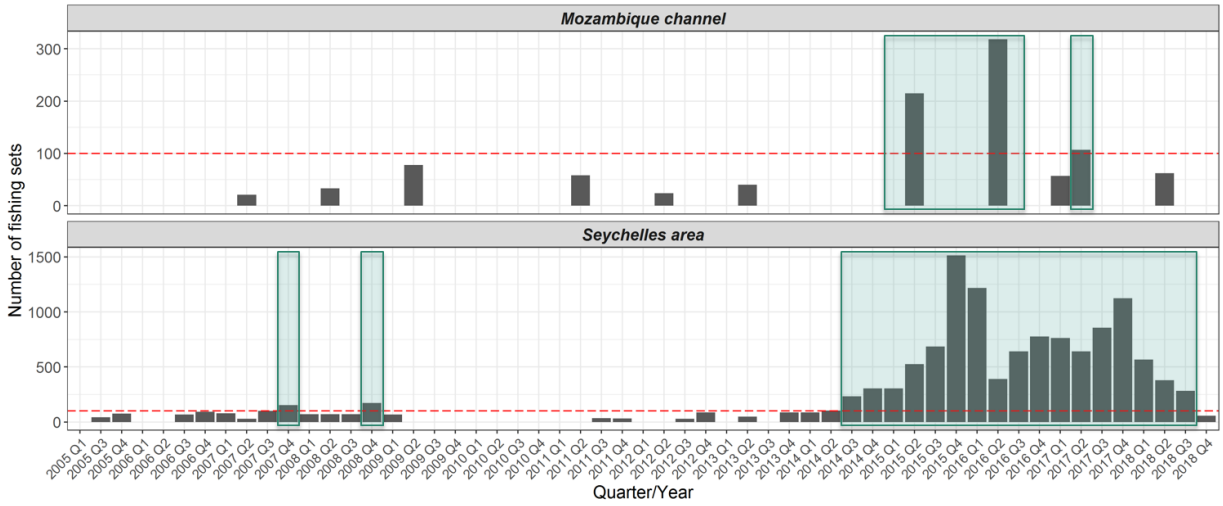

Figure 4. Number of fishing sets available for each statistical unit by area. The red dotted line marks the limit of 100 sets and the blue-shaded areas highlight the catch events distributions that were down-sampled using bootstraps.

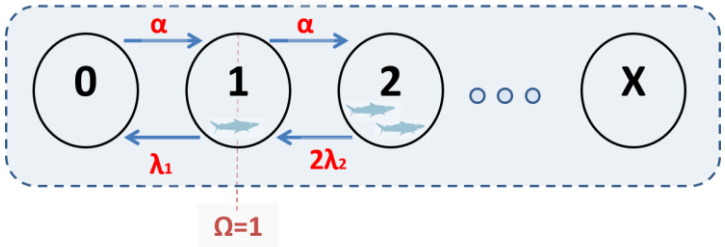

Figure 5. Conceptual model describing the change of state of a FOB in a social scenario. The numbers within each circle represent the number of associated sharks (X). In this example the sociability threshold is equal to 1.

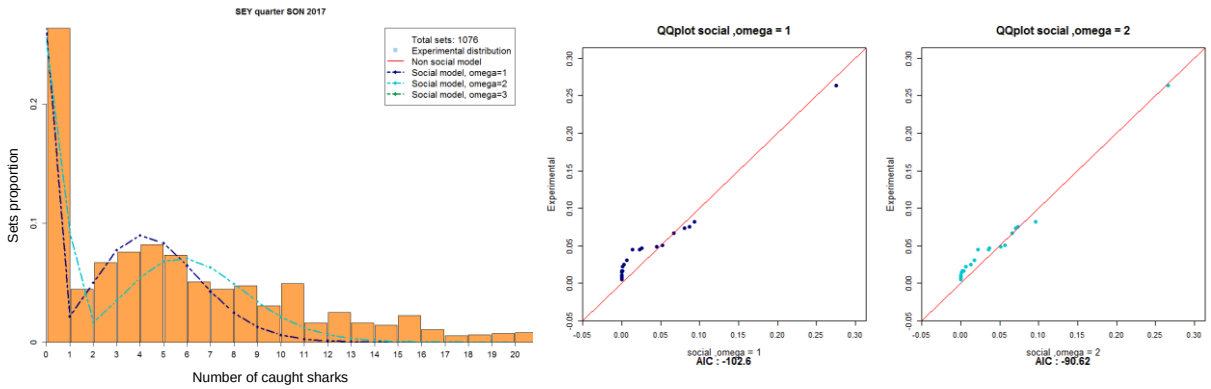

Figure 6. Example of a comparative analysis between two social models fitted to a statistical unit of the Seychelles area (Q4 2017). Left panel illustrates the observed distribution of catch events extracted from the statistical unit. Right panel shows qq-plots and AICs of fitted models. The comparisons were limited to models where all parameters were significant. In this example, the model with a social threshold of 1 provides the best fit.

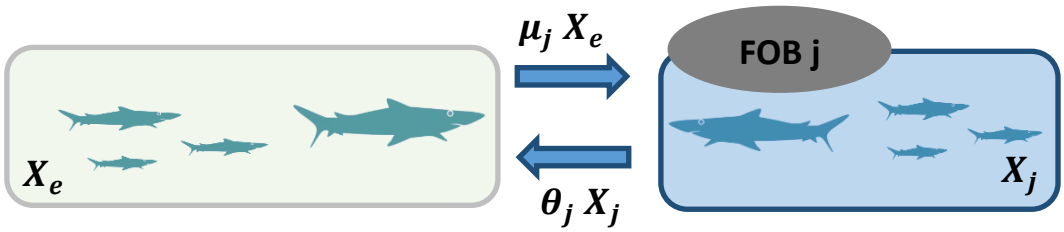

Figure 7. Conceptual model describing the dynamics of silky shark population in a social scenario.

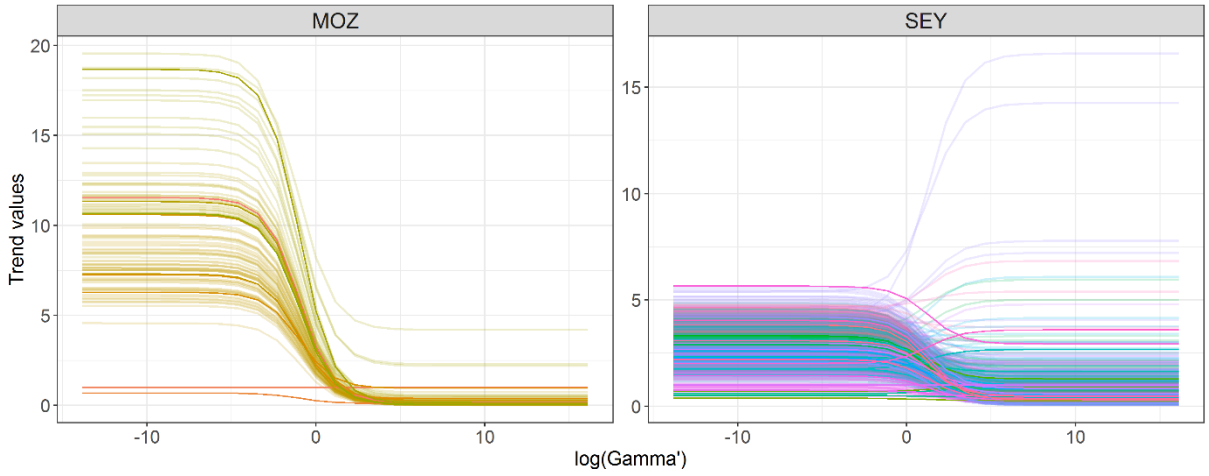

Figure 8. Changes in the abundance trends of silky sharks in the Indian Ocean, following a range of values of γ'. Each color matches a statistical unit or its down-sampled equivalent.

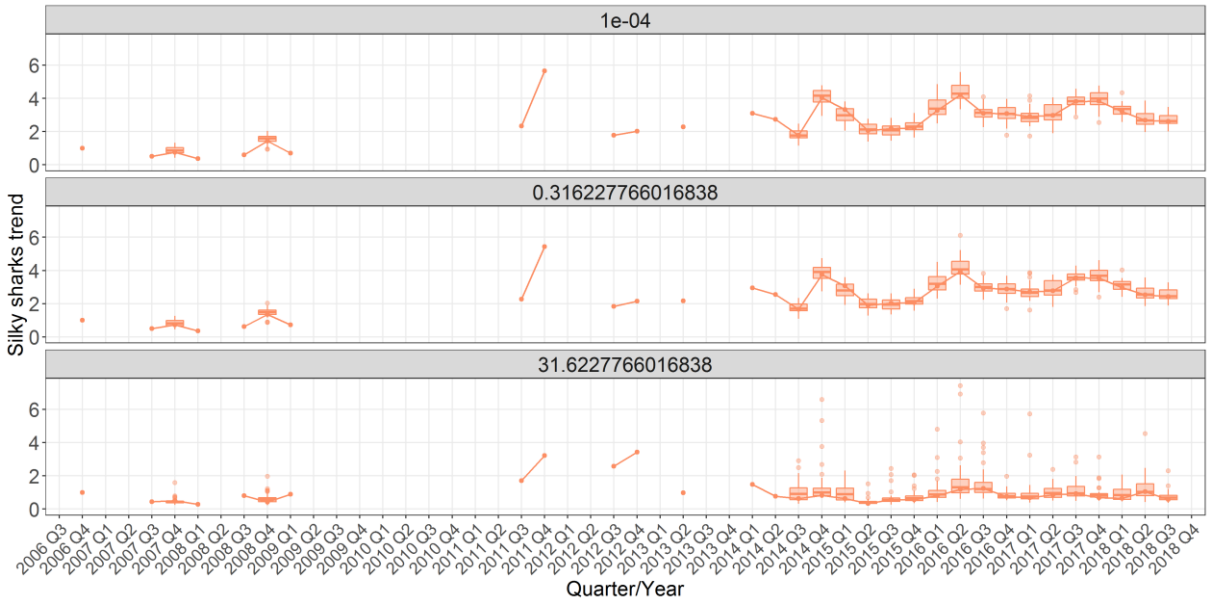

Figure 9. Silky shark abundance trend for the Seychelles area based on three different values of γ'. Solid points represent the index values derived from observed distributions and boxplots represent index values derived from the bootstrapped samples.

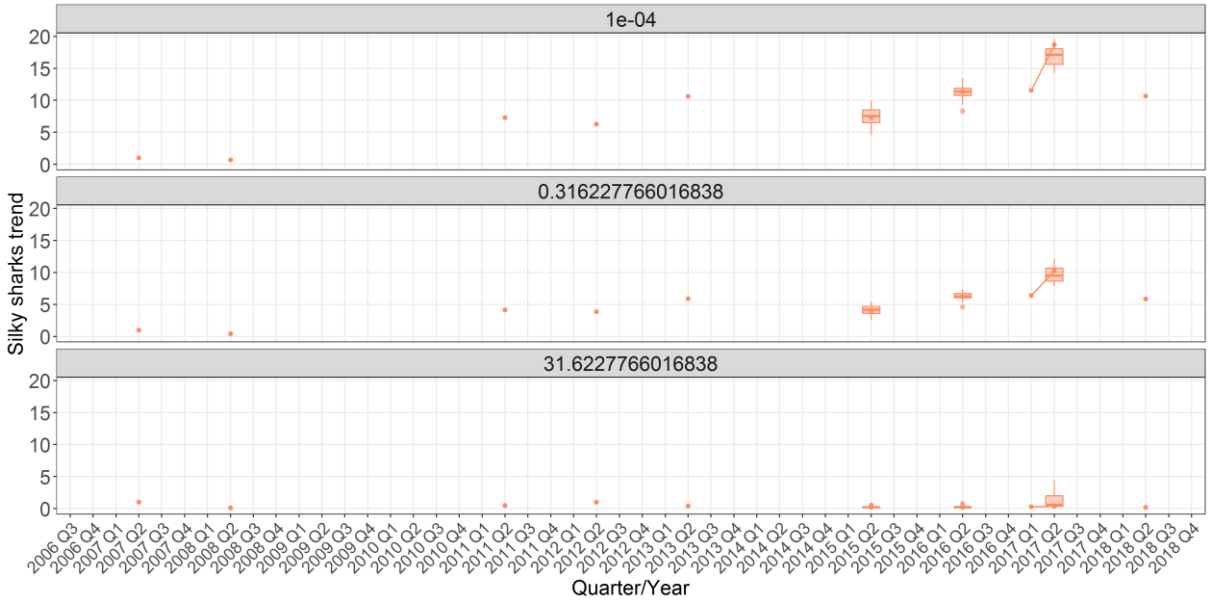

Figure 10. Silky shark abundance trend for the Mozambique Channel area based on three different values of γ'. Solid points represent the index values derived from observed distributions and boxplots represent index values derived from the bootstrapped samples.